

Differential cross section for elastic scattering of electrons from atomic hydrogen: Low energies

P. J. O. Teubner, C. R. Lloyd, and E. Weigold

School of Physical Sciences, The Flinders University of South Australia, Bedford Park, 5042, South Australia

(Received 16 October 1973)

Differential cross sections for the elastic scattering of electrons from atomic hydrogen have been measured at 9.4, 12, and 20 eV. The data at 9.4 eV are shown to agree with a previous measurement and to agree with the prediction of the close-coupling approximation even at the smaller scattering angles of the present experiment. The data at 12 eV agree very well with the six-state close-coupling calculation. The data at 20 eV agree well with a three-state calculation except at the most forward angles.

I. INTRODUCTION

The scattering of electrons from atomic hydrogen has for a long time proven to be of central importance in developing approximations for solving the Coulomb three-body problem. The validity of a particular approximation depends to a large extent on the energy of the incident electron. At low energies, where no or few inelastic channels are open to the scattering process, the close-coupling approximation has proven to be the most reliable of the theoretical treatments.¹ Much of the experimental evidence for the validity of the close-coupling approximation in this energy range comes from measurement of total cross sections for the excitation of the $2p$ state²⁻⁵ and the $2s$ state,⁶⁻⁹ and the polarization of the resonance radiation.¹⁰ Whereas the total-cross-section measurements disagree significantly with the close-coupling calculations,¹ the polarization measurements show good agreement up to the $n=3$ threshold. Since in the total-cross-section measurements the level under investigation is populated in part by cascade from higher states, the discrepancy between theory and experiment may reflect a poor estimate of the contribution to the cross section by cascade.

The angular distributions of elastically scattered electrons do not suffer from ambiguities due to cascade effects and should therefore provide a more reliable test of theory than the inelastic-scattering measurements. At low energies, the only differential elastic-scattering cross-section measurements are those of Gilbody *et al.*,¹¹ whose measurements cover the energy range 3.8–9.4 eV and the angular range 30° – 120° . Total elastic cross sections have also been measured at low energies.¹²⁻¹⁴ Below the excitation threshold the experimental elastic cross-section results are in good agreement with theory. Although the close-coupling approximation predicts the dif-

ferential cross section for scattering angles from 30° to 120° , no data exist outside this angular range and for energies above the first excitation threshold (10.2 eV).

In this paper we report the measurement of the differential cross sections for the elastic scattering of electrons from atomic hydrogen at incident energies of 9.4, 12.0, and 20.0 eV, and compare it with close-coupling calculations. We also describe the modulated beam apparatus and the technique employed in the measurements. In a subsequent paper we will present the results of our investigations at higher energies.

II. EXPERIMENTAL TECHNIQUE

The angular distributions were obtained by observing the electrons elastically scattered from a beam of ground-state hydrogen atoms, produced by dissociating molecular hydrogen in a heated tungsten oven.^{2,15} It can be shown that the dissociated fraction of molecules (D) in such an oven decreases if the gas pressure in the oven is increased. Since the density of neutral particles in the interaction region is proportional to the source pressure, high dissociation implies low target densities. A compromise between the dissociation and the neutral-particle density must be reached.

The dissociation was measured by sampling the neutral beam downstream from the interaction region with a mass spectrometer. Typically, D was between 0.7 and 0.9, corresponding to a significant fraction of molecular hydrogen in the target beam. Thus it was necessary to measure the ratio R of cross sections $\sigma_H(\theta)/\sigma_{H_2}(\theta)$ at each scattering angle and at each energy. This was done using the relation¹³

$$\frac{\sigma_H(\theta)}{\sigma_{H_2}(\theta)} = \frac{1}{\sqrt{2D}} \left| \frac{S_T(\theta)}{S_R(\theta)} \left(\frac{T}{T_R} \right)^{1/2} + D - 1 \right|, \quad (1)$$

where $S_T(\theta)$ is the scattered signal at some tem-

perature T at which the beam is highly dissociated; and $S_R(\theta)$ the scattered signal at a reference temperature T_R where the beam is wholly molecular.

The derivation of this relation assumes that the neutral beam effuses from the source aperture under conditions of molecular flow. Under these conditions, for temperatures below which dissociation occurs, $ST^{1/2}$ is constant. The results of a typical measurement of the elastically scattered signal as a function of the oven temperature are shown in Fig. 1, $\log S$ being plotted versus the $\log T$. The gradient of the straight line is observed to be -0.5 , validating the use of Eq. (1) for determining the cross-section ratio. The furnace was usually operated at about 2800°K , where D was typically 0.85 . The beam temperature, taken to be that of the black-body radiation which emanated from the aperture in the wall of the furnace, was measured with an optical pyrometer. The temperature measurements were corrected for the fact that the furnace aperture was viewed through the chopper wheel, for absorption in the glass window, and for aperture limitations caused by the mass spectrometer. The degree of dissociation was obtained by using the fact that the H_2^+ ion signal as recorded on the mass spectrometer output also obeyed the relation $ST^{1/2} = \text{const.}$ for beam temperatures less than 1500°K . When the beam was dissociated the H_2^+ ion signal decreased more rapidly with temperature than given by this relation. The degree of dissociation can be calculated from the relation

$$1 - D = S_2/S_0, \quad (2)$$

where S_2 is the H_2^+ signal which was recorded at the temperature T and S_0 the signal which would have been found had no dissociation occurred. Figure 1 also shows the variation of the H_2^+ signal with temperature. Although the slope of the straight line is not exactly -0.5 in this case, this does not affect the value of the dissociation obtained from Eq. (2). Thus from measurements of $S_T(\theta)$, $S_R(\theta)$, T , T_R , and D the required atomic to molecular cross-section ratios can be obtained.

Superimposed on $S_T(\theta)$ and $S_R(\theta)$ is a large background signal. This is due to electrons reaching the detector after scattering from the background gas and from parts of the surrounding vacuum chamber. It is well known that by modulating the neutral-particle beam with a mechanical chopper and detecting only the in-phase component of the scattered signal, large noise-to-signal ratios can be tolerated.

A schematic diagram of the apparatus is shown in Fig. 2. Atomic hydrogen was produced by the thermal dissociation of molecular hydrogen in the first of three differentially pumped chambers. A

beam of hydrogen atoms emerged from a 1-mm hole in the wall of the furnace and was modulated at 240 Hz in the second chamber by a rotating toothed wheel. The modulated neutral beam was collimated before passing into the third chamber, where it was crossed with a well-focussed electron beam. The number density of target atoms in the beam was optimized by designing the vacuum system so that the distance between the source and the interaction region was as short as possible (5.5 cm). The time constant of the scattering chamber was approximately 0.5 sec, which was substantially greater than the chopping period thus minimizing errors due to background pressure fluctuations. The base pressure in the scattering chamber was typically 5×10^{-7} torr, which was essentially unaffected by the neutral beam entering the chamber. The composition of the neutral beam was analyzed with a rf quadrupole mass spectrometer and a phase-sensitive detector.

The electron gun, based on the design outlined by Kuyatt,¹⁶ incorporated a Pierce¹⁷ extraction system as the initial electron source. To obtain a well-collimated final beam a fixed-ratio decelerating lens was used. A three-tube variable-ratio-energy-changing lens matched this stage to the source stage. All lens elements were machined from nonmagnetic stainless steel and were accu-

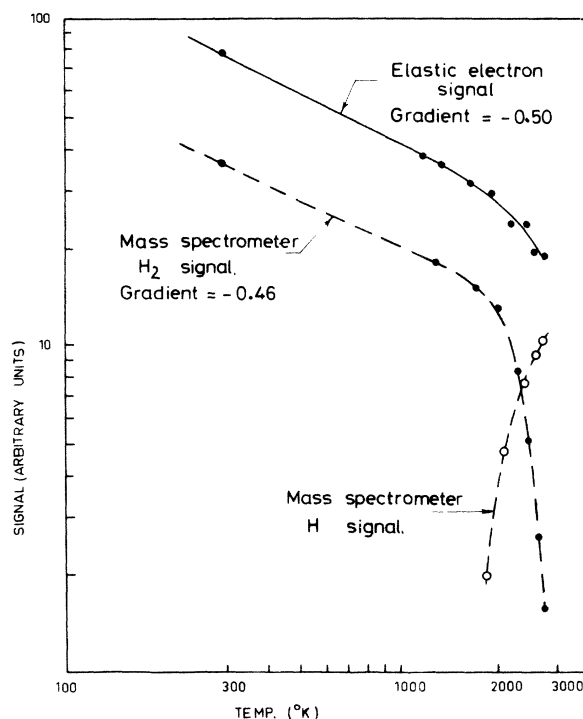


FIG. 1. Temperature dependence of (a) elastically scattered signal at 50° and 20 eV (full line) and (b) mass spectrometer H_2^+ and H^+ signals (dotted lines).

rately located in the gun by sapphire ball spacers. The gun was enclosed in an earthed μ -metal box which served a variety of purposes. It reduced the magnetic field in the gun to less than 20 mG, prevented stray electrons from reaching the spectrometer, and ensured that no stray electric fields from the gun entered the collision region. Final alignment of the electron beam with the target beam was achieved by slightly varying the potential on sets of deflection plates that were situated immediately in front of the gun.

After passing through the interaction region, the electron beam was collected in a Faraday cup consisting of two separately insulated concentric cylinders. The electron beam was focussed by maximizing the current to the center collector, which was 6 mm in diameter, the outer cylinder being 12 mm in diameter. Electrons backscattered from the Faraday cup and reaching the detector were an important source of noise in the experiment. The number of such electrons was reduced by making the front surfaces of the cylinders as thin as possible (0.025 mm) and by coating all surfaces bounding the interaction region with colloidal graphite. The electron beam profile was determined by measuring the current collected in the Faraday cup versus the deflection plate voltage. The angular divergence of the electron beam was less than 0.03 rad. A typical current obtained at 12.0 eV with 90% focussing was $0.25 \mu\text{A}$. The half-width of the energy spread in the beam was estimated to be 0.3 eV.

Both electron gun and Faraday cup were mounted on a rotating table, the axis being formed by the neutral beam. The angular position of the electron beam was determined by reading a scale and a pointer through a window in the vacuum system. A retarding potential analyzer viewed the entire interaction region from a position fixed with respect to the electron gun and collector. This device selected those electrons which had been scattered elastically from the neutral beam. The solid angle subtended by the analyzer was sufficiently large so that the scattering volume remained independent of the scattering angle. The angular resolution using this arrangement was 3° with an energy resolution of less than 1 eV. The retarding-field type of spectrometer is well suited for the selection of elastically scattered electrons, as its action is that of a high-pass energy filter. Another advantage is that a large acceptance angle could be obtained easily with constant transmission characteristics across that angle. Its main disadvantage was that photons from excited atoms in the interaction region were able to reach the electron detector (Channeltron). Thus for energies above the first excitation threshold for atomic and molecular hydrogen, the modulated beam signal contained a component which arose from the excitation of vacuum uv photons. This component was resolved from the electron signal by reducing the potential on the spectrometer to a value less than that of the incident beam. The signal which was then detected was attributed to photons and

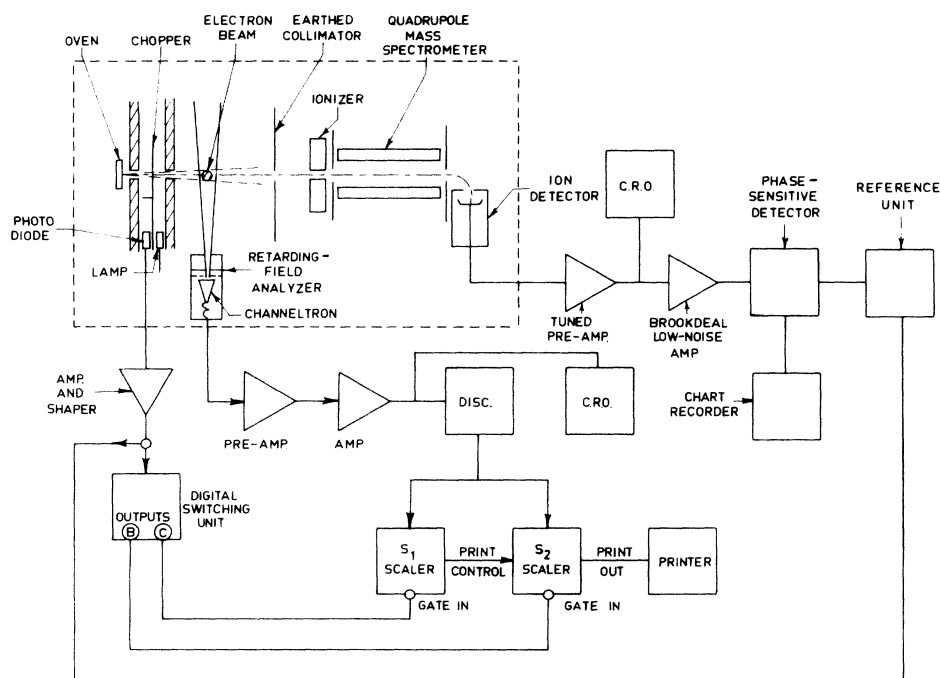


FIG. 2. Schematic diagram of the apparatus.

was subtracted from the signal recorded under normal conditions. This correction for photons was always much less than 1% of the elastic signal for electron energies equal to or less than 20 eV. The symmetry of the angular distributions was verified by taking data at both positive and negative scattering angles. The possibility of the earth's magnetic field influencing the shape of the distributions was reduced by using a set of Helmholtz coils to balance out the earth's field. The residual field near the interaction region was measured to be below 50 mG. The maximum deviation in scattering angle that could be caused by this residual field was calculated to be considerably smaller than the angular resolution. The interaction region was shielded from the magnetic field due to the high oven current by surrounding the oven chamber with netic A.A.

After passing through the retarding-field analyzer, the elastically scattered electrons were detected in a Channeltron. The output pulses from the Channeltron were processed by a digital phase-sensitive detection system in order to separate the beam component from the background noise. This was accomplished by gating two scalers so that one was on only when the beam was on, and

the other on only when the beam was off. By routing the Channeltron output into both scalers, scaler 1 recorded the counts produced by electrons elastically scattered from the beam plus background, while scaler 2 recorded only the background counts. The gating signal was obtained from a digital delay unit, triggered by a photodiode that was illuminated by a light source on the opposite side of the mechanical chopper. A timing circuit controlled by a 10-MHz crystal clock allowed the reference signal to be delayed by a preset interval. A second timing circuit controlled by the same clock allowed the mark-space ratio to be varied. Two outputs, 180° out of phase with each other, were then used to gate the two scalers on and off in synchronism with the beam signal. It was important to have accurate stable switching times so that adverse signal-to-noise ratios could be handled adequately. The switching accuracy depended on whether the "on" times for each scaler were equal. The 10-MHz clock with ± 2 -Hz uncertainty resulted in a timing precision of 0.01%.

The electron beam current was maintained constant to within 0.2% during the taking of data, and the neutral-particle beam was monitored with the mass spectrometer so that drifts in intensity could be corrected for. The main source of error in the data was then the statistical counting error. Dead-

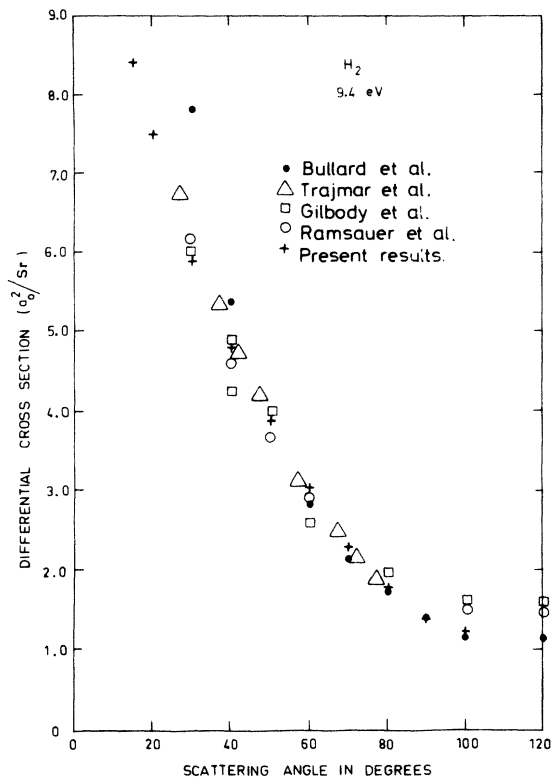


FIG. 3. Elastic e - H_2 differential cross sections at 9.4 eV. The data of Bullard *et al.*, Trajmar *et al.*, and Ramsauer *et al.* were taken at 10 eV.

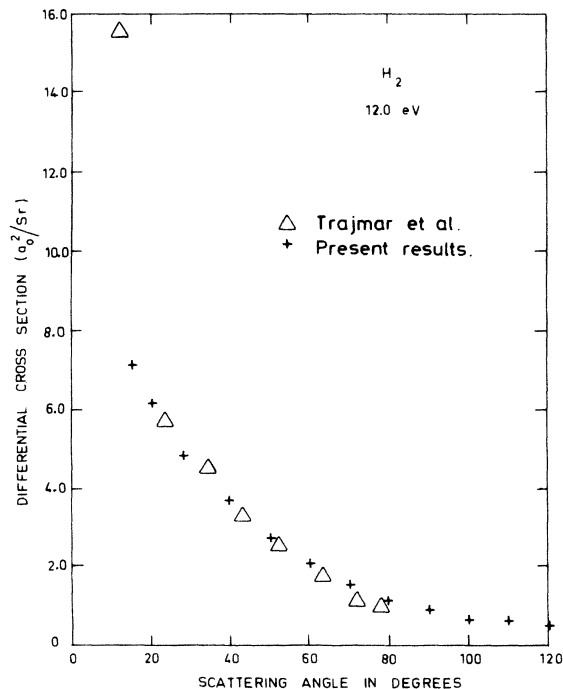


FIG. 4. Elastic e - H_2 differential cross section at 12.0 eV.

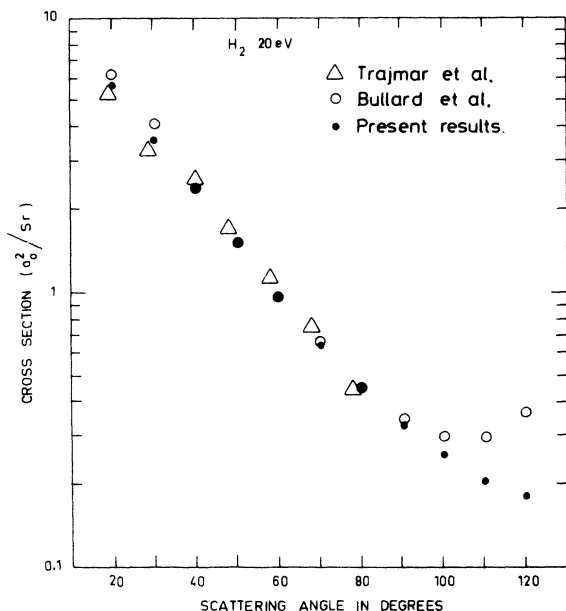


FIG. 5. Elastic $e\text{-H}_2$ differential cross section at 20.0 eV.

time corrections were not necessary, as the count rates were always less than 1 kHz.

III. RESULTS AND DISCUSSION

A. Molecular hydrogen

Angular distributions for the low-energy scattering of electrons from molecular hydrogen have been measured by many workers.^{18,19,11} Of these only Ramsauer and Kollath¹⁸ and Trajmar *et al.*¹⁹ attempted to give absolute values. The highest

TABLE I. The ratio $R = \sigma_{\text{H}}(\theta)/\sigma_{\text{H}_2}(\theta)$ for elastic scattering of electrons by atomic and molecular hydrogen as a function of angle and incident energy.

Scattering angle (deg)	9.4 eV	12.0 eV	20.0 eV
15		0.61 ± 0.03	0.58 ± 0.02
20	0.63 ± 0.04	0.62 ± 0.03	0.58 ± 0.02
30		0.57 ± 0.03	0.54 ± 0.03
40	0.57 ± 0.03	0.57 ± 0.035	0.53 ± 0.03
50		0.555 ± 0.04	0.57 ± 0.035
60		0.55 ± 0.04	0.61 ± 0.03
70	0.70 ± 0.04	0.66 ± 0.04	0.71 ± 0.03
80		0.74 ± 0.04	0.775 ± 0.035
90	0.81 ± 0.05	0.78 ± 0.06	0.87 ± 0.04
100		0.85 ± 0.08	0.98 ± 0.05
110			0.97 ± 0.06
120			1.00 ± 0.07
135			0.98 ± 0.10

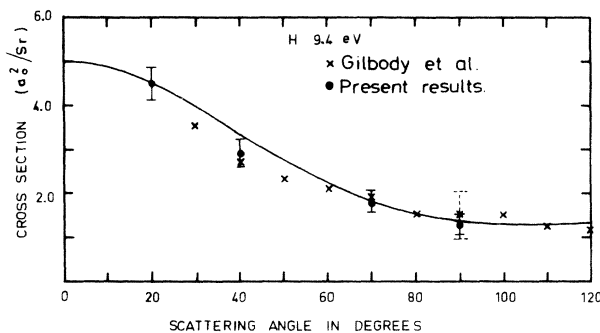


FIG. 6. Elastic $e\text{-H}$ differential cross section at 9.4 eV. Dots with error bars show the present data. Crosses show the data of Gilbody *et al.*¹¹ with their error indicated 90°. The full line gives the results of the close-coupling calculations (Ref. 21).

incident electron energy used by Ramsauer and Kollath was only 10.0 eV, whereas Trajmar *et al.* measured differential cross sections from 10° to 80° scattering angle for impact energies of 7, 10, 13.6, 20, 45, 60, and 81.6 eV. At 20 eV and below, these results were normalized using the total $e\text{-H}_2$ elastic-scattering data of Golden *et al.*,²⁰ with an error estimated to be $\pm 35\%$. This value included the error in the normalization procedure as well as experimental uncertainties. Figures 3 to 5 show the present results compared with other experimental results. Normalization of the present results was achieved by using the absolute H_2 values of Trajmar *et al.*, the data

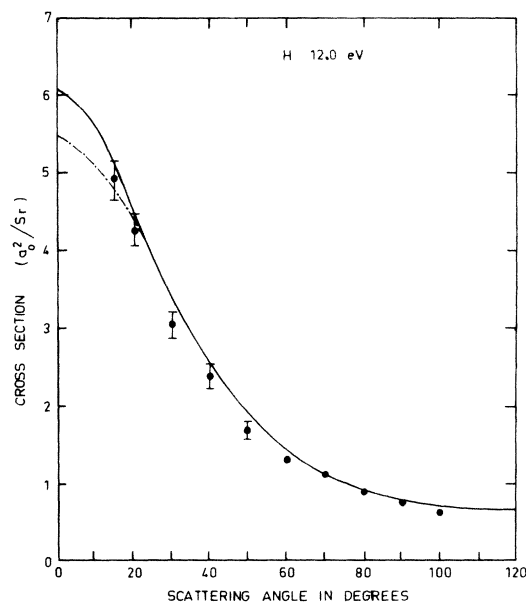


FIG. 7. Elastic $e\text{-H}$ differential cross section at 12.0 eV. The full line gives the results of the six-state close-coupling calculation (Ref. 22), the broken line that of the three-state calculation (Ref. 21).

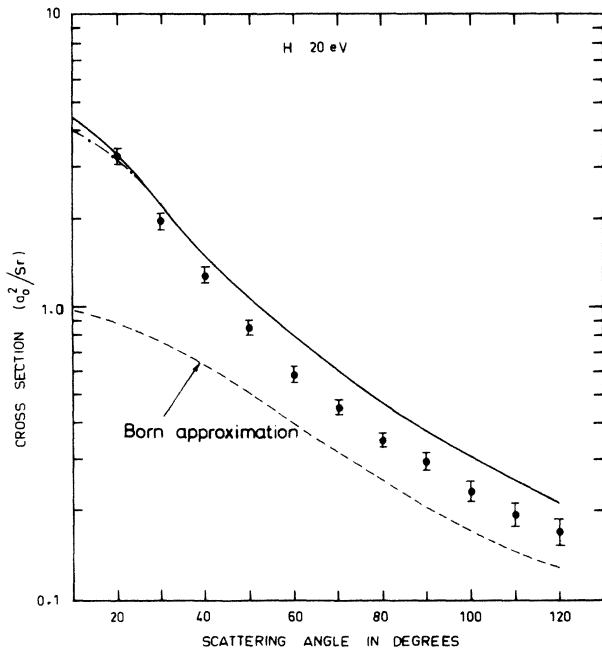


FIG. 8. Elastic e -H differential cross section at 20.0 eV. The full line gives the three-state close-coupling results of Scott (Ref. 23), and the broken line the results obtained by Burke *et al.* (Refs. 21 and 22). The results of the Born approximation are also shown for comparison.

at 9.4 and 12.0 eV being normalized by interpolation. All other relative experimental angular distributions except those of Ramsauer and Kollath were then normalized to the present results for the best visual fit. The relative errors in the present data are less than 2% at all angles. In general, the earlier scattering results¹⁸ do not agree well with the present results and with those of Trajmar *et al.*, the main discrepancy occurring at backward angles. However, the present results are in good agreement with the results of Trajmar *et al.*¹⁹ and Gilbody *et al.*²⁰

B. Atomic hydrogen

The ratios R of electrons elastically scattered from atomic hydrogen to those elastically scattered from molecular hydrogen at different angles

and energies are shown in Table I. The errors here quoted correspond to one standard deviation and arise from the statistical sum of errors in S_T , S_R , T , T_R , and D . These ratios were converted into differential cross sections for the elastic scattering of electrons from atomic hydrogen by forming the product $R\sigma_{1/2}(\theta)$. The resulting cross sections are shown in Figs. 6, 7, and 8. At 9.4 eV there is good agreement in both shape and absolute value with the previous measurement of Gilbody *et al.*, which was normalized to the earlier data of Ramsauer and Kollath. At 90° Gilbody *et al.* obtained the value of 0.83 ± 0.16 for R , in excellent agreement with the more-accurate present value of 0.81 ± 0.05 . The close-coupling calculation²¹ still fits the data at a scattering angle of 20°.

The differential cross section at an incident energy of 12.0 eV is shown in Fig. 7. No previous measurements exist at this energy. The results compare very well in shape and absolute value with the close-coupling calculations of Burke *et al.*^{21,22} The difference between the three-state and the six-state close-coupling calculations is significant only for angles less than 30°. The present data are not sufficiently accurate to discriminate between the two calculations, as both fit the data to within the experimental error.

At 20.0 eV (Fig. 8) the close-coupling calculations^{21,23} give the shape of the observed angular distribution for scattering angles greater than 30°. The discrepancy in absolute value could be due to the 35% error in normalization.¹⁹ The full line in Fig. 8 represents the results obtained by Scott,²³ who used the three-state close-coupling reactance matrix elements of Burke *et al.*²¹ supplemented by Born-approximation values for higher partial waves. The broken line represents the results obtained using Burke's original data.

ACKNOWLEDGMENTS

The authors are grateful to the Australian Research Grants Committee for financial assistance and to B. Bridger and B. Hewitt for assistance in construction of the apparatus.

¹S. Geltman, *Invited Papers, Seventh International Conference on the Physics of Electronic and Atomic Collisions* (North-Holland, Amsterdam, 1972), p. 216.

²W. L. Fite and R. T. Brackmann, *Phys. Rev.* **112**, 1141 (1958).

³R. L. Long, D. M. Cox, and S. J. Smith, *J. Res. Natl. Bur. Stand. (U.S.) A* **72**, 521 (1968).

⁴J. W. McGowan, J. F. Williams, and D. K. Curley,

Phys. Rev. **180**, 132 (1969).

⁵G. E. Chamberlain, S. J. Smith, and D. W. O. Heddle, *Phys. Rev. Lett.* **12**, 647 (1964).

⁶W. Lichten and S. Schultz, *Phys. Rev. Lett.* **116**, 1132 (1959).

⁷R. F. Stebbings, W. L. Fite, D. G. Hummer, and R. T. Brackmann, *Phys. Rev.* **119**, 1939 (1960).

⁸D. Hils, H. Kleinpoppen, and H. Koschmieder, *Proc.*

- Phys. Soc. 89, 35 (1966).
- ⁹W. Kauppila, W. R. Ott, and W. L. Fite, Phys. Rev. A 1, 1099 (1970).
- ¹⁰W. R. Ott, W. E. Kauppila, and W. L. Fite, Phys. Rev. A 1, 1089 (1970).
- ¹¹H. B. Gilbody, R. F. Stebbings, and W. L. Fite, Phys. Rev. 121, 794 (1961).
- ¹²B. Bederson, H. Malamad, and J. Hammer, Bull. Am. Phys. Soc. 2, 122 (1957).
- ¹³R. G. Brackmann, W. L. Fite, and R. H. Neynaber, Phys. Rev. 112, 1157 (1958).
- ¹⁴R. Neynaber, L. L. Marino, E. W. Rothe, and S. M. Trujillo, Phys. Rev. 124, 135 (1961).
- ¹⁵W. E. Lamb and R. C. Retherford, Phys. Rev. 79, 549 (1950).
- ¹⁶C. E. Kuyatt, Lecture Notes (Electron Optics, unpublished) (1967).
- ¹⁷J. R. Pierce, *Theory and Design of Electron Beams* (Van Nostrand, Princeton, N. J., 1954).
- ¹⁸C. Ramsauer and R. Kollath, Proc. Roy. Soc. Lond. A 133, 637 (1932); E. C. Bullard and H. S. W. Massey, Proc. Roy. Soc. Lond. A 130, 637 (1931); A. L. Hughes, and J. H. McMillen, Phys. Rev. 41, 154 (1932); G. M. Webb, Phys. Rev. 47, 379 (1935).
- ¹⁹S. Trajmar, D. G. Truhlar, and J. K. Rice, J. Chem. Phys. 52, 4502 (1970).
- ²⁰D. E. Golden, H. W. Bandel, and J. A. Salerno, Phys. Rev. 146, 40 (1966).
- ²¹P. G. Burke, H. M. Schey, and K. Smith, Phys. Rev. 129, 1258 (1963).
- ²²P. G. Burke, S. Ormonde, and W. Whitaker, Proc. Phys. Soc. 92, 319 (1967).
- ²³B. L. Scott, Phys. Rev. 140, A699 (1965).